

High Resolution Spectroscopy of 4U 1728-34 from a Simultaneous Chandra-RXTE Observation

A. D'Alí*, T. Di Salvo*, R. Iaria*, G. Lavagetto*, N. R. Robba*, L. Burderi†,
M. Mendez** and M. van der Klis‡

*Dipartimento di Scienze Fisiche ed Astronomiche, Università di Palermo, via Archirafi n.36,
90123 Palermo, Italy.

†Osservatorio Astronomico di Roma, Via Frascati 33, 00040 Monteporzio Catone (Roma), Italy.

**SRON National Institute for Space Research, Sorbonnelaan 2, 3584 CA Utrecht, the Netherlands

‡Astronomical Institute "Anton Pannekoek," University of Amsterdam and Center for High-Energy
Astrophysics, Kruislaan 403, NL 1098 SJ Amsterdam, the Netherlands

Abstract. We report on a simultaneous Chandra and RossiXTE observation of the LMXB atoll bursting source 4U 1728-34 performed on 2002 March 3–5. We fitted the 1.2–35 keV continuum spectrum with a blackbody plus a Comptonized component. An overabundance of Si by a factor of ~ 2 with respect to Solar abundance is required for a satisfactory fit. Large residuals at 6–10 keV can be fitted by a broad (FWHM $\simeq 1.6$ keV) Gaussian emission line, or, alternatively, by absorption edges associated with Fe I and Fe XXV at ~ 7.1 keV and ~ 9 keV, respectively. In this interpretation, we find no evidence of broad, or narrow Fe K α line, between 6 and 7 keV. We tested our alternative modeling of the iron K α region by reanalyzing a previous BeppoSAX observation of 4U 1728-34, finding a general agreement with our new spectral model.

Keywords: accretion discs – stars: individual: 4U 1728-34 — stars: neutron stars — X-ray: stars — X-ray: spectrum — X-ray: general

PACS: 97.80.Jp

INTRODUCTION

4U 1728-34 is a well known prototype of the class of the bursting atoll sources ([4]). This was one of the first sources to display kHz QPOs in its power spectrum and the first one to display burst oscillations, around 363 Hz, during some type I X-ray bursts ([7]). Its temporal behavior has been recently extensively studied ([2], [10]) using a large set of RXTE observations, spanning more than three years. Spectral studies have been carried out in the past with the use of EXOSAT ([11]), RXTE ([6]) and BeppoSAX ([1], [6]) satellites; although there was a general agreement about the modelization of the continuum emission, it was disputed the nature of local features, especially a broad Gaussian line at 6.2-6.7 keV. The distance to the source is estimated between 4.1 kpc and 5.1 kpc ([3]; [1]).

In this paper we present the results from a simultaneous Chandra-RXTE observation of 4U 1728-34. We propose an alternative fit of the iron K-shell region, using two absorption edges instead of a broad emission line, whose interpretation would be quite problematic.

OBSERVATIONS AND SPECTRAL ANALYSIS

4U 1728-34 was observed by Chandra on 2002 March 4 for a total collecting time of ~ 30 ksec. We used the Chandra High Energy Transmission Grating Spectrometer (HETGS) to perform a high resolution spectroscopic analysis. The data were collected in the Timed Exposure Mode, and a sub-array was adopted ($q = 1$ and $n = 400$, see the Chandra Proposer's Observatory Guide at <http://cxc.harvard.edu/proposer/POG>) in order to mitigate the effects of photon pile-up for first order spectra. Consequently the frame time was 1.44 s, the High Energy Grating (HEG) spectrum is cut below 1.6 keV and the Medium Energy Grating (MEG) spectrum below 1.2 keV. No systematic error was added to the data. The RXTE observation started on 2002 March 3 03:27:12 and ended on 2002 March 5 13:00:00. For the spectral analysis we used only the Proportional Counter Units 2 and 3 data in the Standard2 configuration (with 16 s time resolution and 129 energy channels). Seven type-I bursts were revealed in the PCA lightcurve and two bursts in the Chandra lightcurve. As our primary concern is to focus on the persistent emission of the source we discarded data around each burst, for a time length of 160 s.

As concerns the Chandra HETG data, we considered the four first-order dispersed spectra, namely the two HEG spectra and the two MEG spectra on the opposite sides of the zeroth order. We averaged HEG+1 (MEG+1) and HEG-1 (MEG-1) spectra in a single spectrum, after having tested their reciprocal consistency. The used energy range is 1.6-10 keV for the HEG spectrum and 1.2-5 keV for the MEG spectrum. For all the fits we took into account an instrumental feature at 2.07 keV for bright sources (described by [5]) and fit it with an inverse edge (with optical depth $\tau \simeq -0.1$). The HEG and MEG spectra were binned in order to have at least 300 counts for each bin. This, however, still ensures a high number of channels (about 1000) and good spectral resolution throughout the entire covered energy band. Concerning the RXTE/PCA data the standard selection criteria for obtaining the Good Time Intervals were applied. We restricted the spectral analysis to the temporal intervals during which RXTE operated simultaneously with Chandra. We limited the energy range to 3.5-35 keV, and applied a 2% systematic error for channels below 25 keV and 2.5% for channels above 25 keV. Relative normalizations of the three instruments, except for HEG which was fixed to a reference value of 1, were left as free parameters in all the fits performed.

We tried a series of models to simultaneously fit HEG, MEG and RXTE spectra. We found the best-fit model to consist of a soft emission, described by a blackbody of temperature $\simeq 0.52$ keV, plus a Comptonized component (CompTT in XSPEC, [8]), where the seed photon temperature kT_0 is $\simeq 1.3$ keV, the electron temperature kT_e is $\simeq 7.4$ keV and, finally, the optical depth τ associated to a spherical corona is $\simeq 6.2$. Both components are photo-electrically absorbed by an equivalent hydrogen column $N_H \simeq 2.3 \times 10^{22} \text{ cm}^{-2}$. The associated $\chi^2/\text{d.o.f.}$ obtained for this fit is 1206/1034. We noted an evident absorption edge around 1.84 keV, probably associated to neutral Si, in the MEG and HEG spectra. To fit this edge we substituted the component *phabs* in XSPEC with the component *vphabs*, which allows us to vary the abundances of single elements with respect to the solar abundances. We found that leaving the Si abundance free improves the fits significantly; Si resulted overabundant by a factor ~ 2 with respect to the solar abundance ($\chi^2/\text{d.o.f.}$ value obtained for this fit is 1031/1033).

Large residuals at 6–10 keV can be fitted by a very broad Gaussian emission line

($\sigma \simeq 0.7$ keV, corresponding to a FWHM $\simeq 1.6$ keV), whose interpretation is quite problematic, or, alternatively, by absorption edges associated with Fe I and Fe XXV at 7.03 keV ($\tau \simeq 0.11$) and ~ 9 keV ($\tau \simeq 0.16$, respectively). The addition of these edges improves the fit significantly compared to the simple model described above (giving a decrease of $\chi^2/\text{d.o.f.}$ from 1031/1033 to 959/1029). In this interpretation, we find no evidence of broad, or narrow Fe K α line, between 6 and 7 keV. To test the consistency of our model we reanalyzed a previous BeppoSAX observation performed between August 23 and 24, 1998 (see [1]). A Gaussian emission line is no longer statistically required if we introduce two absorption edges at energies above 7 keV. We found a first edge at $\simeq 7.4$ keV ($\tau \simeq 0.08$) and a second edge at $\simeq 8.7$ keV ($\tau \simeq 0.06$). We found a general agreement with the Chandra-RXTE spectrum, obtaining $\chi^2/\text{d.o.f.} = 225/179$ (instead of $\chi^2/\text{d.o.f.} = 236/178$ obtained for the model adopted in [1]). In table 1 and Figure 1 we present the results of the two fits of the BeppoSAX and Chandra-RXTE datasets.

CONCLUSIONS

We confirm that the best-fit continuum model for this source is composed of two components: a blackbody emission which probably comes from the inner edge of an accretion disk around the compact object, and a Comptonized component coming from a hot corona surrounding the system. Although we cannot definitely exclude that a quite broad Gaussian line ($\sigma \simeq 0.7$ keV, FWHM $\simeq 1.6$ keV) is present in this source, we present here a different interpretation of the residuals in the iron K-shell region. These are well fitted by two absorption edges at energies at ~ 7 and ~ 9 keV, associated with Fe I and Fe XXV, respectively (see e.g. [9]). We derived, however, an upper limit to the flux of a broad emission line, fixing the values of energy and width to the values found in [1]; we find an upper limit to the line flux of 1.7×10^{-11} erg cm $^{-2}$ sec $^{-1}$ (corresponding to an equivalent width of 28 eV).

We checked that this alternative model is also in agreement with a previous BeppoSAX observation. We observe a shift in the energy of the Fe I edge from 7.1 keV during the Chandra-RXTE observation to 7.4 keV (compatible with K α edges of moderately ionized iron, Fe IX to Fe XVI) during the BeppoSAX observation, while the energy of the Fe XXV edge is consistent with being the same in both observations. Finally we found, both in the Chandra-RXTE and BeppoSAX spectra, a Si overabundance by a factor $\sim 2 - 2.5$ with respect to the solar abundance and the values obtained from the fit are consistently in agreement.

REFERENCES

1. Di Salvo T., Iaria R., Burderi L., Robba N.R., 2000, ApJ, 542, 1034
2. Di Salvo T., Mendez M., van der Klis M., Ford E., Robba N.R., 2001, ApJ, 546, 1107
3. Galloway D.K., Psaltis D., Chakrabarty D., Munro M.P., 2003, ApJ, 590, 999
4. Hasinger, G., & van der Klis, M., 1989, A&A, 225, 79
5. Miller J.M., Fabian A.C., Wijnands R., et al., 2002, ApJ, 578, 450
6. Piraino S., Santangelo A., Kaaret P., 2000, A&A, 360, L35
7. Strohmayer T.E., Zhang W., Swank J.H., et al., 1996, ApJ, 469, L9
8. Titarchuck L., 1994, ApJ, 434, 570

TABLE 1. Best fit parameters for the two datasets of 4U 1728-34, obtained from a BeppoSAX observation (0.12-60 keV energy band) and a joint CHANDRA-RXTE observation (1.2-35 keV energy band). The continuum emission consists of a thermal blackbody (bbody) and a Comptonized component modeled by compTT. kT_{BB} and N_{BB} are, respectively, the blackbody temperature and normalization in units of L_{39}/D_{10}^2 , where L_{39} is the luminosity in units of 10^{39} ergs/s and D_{10} is the distance in units of 10 kpc. kT_0 , kT_e and τ indicate the seed-photon temperature, the electron temperature and the optical depth of the Comptonizing cloud around the neutron star. N_{CompTT} is the normalization of the CompTT model in XSPEC v.11.2.0 units. Unabsorbed luminosities of the bbody component and of the CompTT component are calculated assuming a distance to the source of 5.1 kpc ([1]). For the component Edge, E_{edge} denotes the energy of the edge and τ the optical depth. Uncertainties are at 90% confidence level for a single parameter.

		BeppoSAX	Chandra - RXTE
Component	Parameter (Units)	Values	
vpha	N_{H} (10^{22} cm $^{-2}$)	$2.37^{+0.14}_{-0.11}$	$2.61^{+0.06}_{-0.07}$
vpha	Si (Solar units)	$2.1^{+0.5}_{-0.5}$	$2.02^{+0.13}_{-0.13}$
edge	E_{edge} (keV)	$7.41^{+0.15}_{-0.14}$	$7.03^{+0.08}_{-0.06}$
edge	τ (10^{-2})	8^{+2}_{-2}	11^{+3}_{-4}
edge	E_{edge} (keV)	$8.73^{+0.26}_{-0.24}$	$9.0^{+0.3}_{-0.4}$
edge	τ (10^{-2})	6^{+3}_{-3}	16^{+4}_{-4}
bbody	kT (keV)	$0.573^{+0.002}_{-0.024}$	$0.516^{+0.002}_{-0.014}$
bbody	N_{BB} (10^{-3})	$21.5^{+1.6}_{-1.3}$	$10.3^{+0.4}_{-0.4}$
bbody	Luminosity (10^{36} erg cm $^{-2}$ sec $^{-1}$)	5.7	0.87
CompTT	kT_0 (keV)	$1.53^{+0.06}_{-0.07}$	$1.33^{+0.05}_{-0.05}$
CompTT	kT_e (keV)	$6.4^{+1.3}_{-0.4}$	$7.4^{+0.5}_{-0.4}$
CompTT	τ	$4.8^{+0.8}_{-1.0}$	$6.2^{+0.4}_{-0.6}$
CompTT	N_{CompTT} (10^{-2})	$6.8^{+1.3}_{-1.4}$	$4.4^{+0.3}_{-0.6}$
CompTT	Luminosity (10^{36} erg cm $^{-2}$ sec $^{-1}$)	10.2	2.6
χ^2/dof		225/179	959/1029

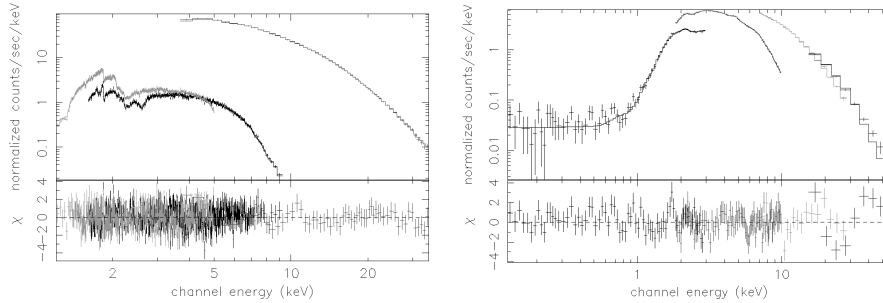


FIGURE 1. Spectra of 4U 1728-34 shown together with the best-fit model (see Table 1). Left panel: 1.2–35.0 keV spectrum obtained from the simultaneous Chandra and RXTE dataset. Right panel: 0.12–60 keV spectrum obtained from a BeppoSAX observation. In smaller panels: residuals in unit of σ with respect to the best-fit model.

9. Turner T.J., Done C., Mushotzky R., Madejski G., Kunieda H., 1992, ApJ, 391, 102
10. van Straaten S., van der Klis M., Di Salvo T., Belloni T., 2002, ApJ, 568, 912
11. White N.E., Peacock A., Hasinger G., et al., 1986, MNRAS, 218, 129